# MODELING SPATIAL TREE PATTERNS IN THE TAPAJÓS FOREST USING INTERFEROMETRIC HEIGHT

**Till Neeff[1,2]**
**Gregory S. Biging[3]**
**Luciano V. Dutra[1]**
**Corina C. Freitas[1]**
**João R. dos Santos[1]**

**[1]Instituto Nacional de Pesquisas Espaciais - INPE**
**Earth Observation Area - OBT**
Av. dos Astronautas, 1758; 12.227-010 São José dos Campos (SP); Brazil
{dutra, corina}@dpi.inpe.br, jroberto@ltid.inpe.br

**[2]University of Freiburg**
**Biometry Department**
Tennenbacher Straße 4; 79085 Freiburg Brsg.; Germany
tillneeff@fulbrightweb.org

**[3]University of California at Berkeley**
**Center for Assessment and Monitoring of Forest and Environmental Resources - CAMFER**
227 Mulford Hall; Berkeley, CA 94720; USA
biging@nature.berkeley.edu

## ABSTRACT

The spatial distribution of very large trees in primary Amazon forest is extracted from a digital model of interferometric forest height by an approach of local maximum filtering. The spatial point patterns of very large trees are modeled by a series of Markov point process models. Spatial distribution is regular, and interaction decreases with distance; very large trees are shown to exert repulsive interaction with their neighboring very large trees.

**Keywords:** InSAR, K-function, Local maximum filtering, Markov process, primary forest, spatial point pattern.

## RESUMO

A distribuição espacial de árvores muitas altas em florestas primárias na Amazônia é extraída de um modelo digital interferométrico da altura do dossel florestal, através de uma filtragem de máximas locais. Os padrões pontuais espaciais de árvores muito altas são modelados por uma série de modelos de processos pontuais de Markov. As distribuições espaciais são regulares, e as interações decrescem com a distância; é mostrado que árvores muito altas exercem interações repulsivas com árvores vizinhas muito altas.

**Palavras chave:** InSAR, função K, filtragem de máximas locais, processo de Markov, floresta primária, padrão espacial pontual.

### 1. INTRODUCTION

In ecological forest studies, some researchers have paid special attention to a sub-collective of only the largest trees. A particular ecological significance for the carbon regime, patterns of succession, and species diversity is attributed to very large trees. CHAMBERS *et al*. (2001) depict that in tropical forests half of the above-ground biomass is contained in very few tree individuals. MILTON *et al.* (1994) characterize very large trees in tropical forests as reproductively dominant, and therefore strongly influential on forest structure and composition. In this paper, trees with dominant crown position are very large trees (VLTs), that therefore appear in data from radar interferometry (see NEEFF *et al*., 2005a).

Three-dimensional stand structure has been called “the most important of all stand characteristics”

for determining its biodiversity and ecological stability (PRETZSCH, 1997). Stochastic point process have been identified as the appropriate tool for examining spatial structure of trees in temperate and tropical forests (e.g. PRETZSCH, 1997; STOYAN AND PENTTINEN, 2000).

## 2. MATERIAL AND METHODS

### 2.1 Study area

The study area is situated in the surroundings of the Tapajós National Park south of Santarém in Brazilian Amazonia at W 54.93 DD, and S 3.19 DD. The climate according to Köppen is *Amw* (variation of tropical monsoon) with an average annual rainfall of ca. 1,850 mm, and a yearly temperature average of 26 °C. Hence, the life zone is classified as *tropical moist forest* according to the Holdrige system.

### 2.2 Remote sensing data

An area of approximately 1,300 $km^2$ was mapped at the end of 2000. The data were collected by the airborne AeS-1 sensor (Aerosensing Radarsysteme GmbH, Germany), which makes use of interferometric synthetic aperture radar (InSAR) technology. It operates on X-band (9.55 GHz) with one polarization (HH) and fully polarimetric on P-band (technical properties: wavelength 72 cm; middle frequency 415 MHz; depression angle 45° (37-51°); mean flight height 3,216 m; range resolution 1.5 m; azimuth resolution 0.7 m for 1 look slant range image).

The longer wavelengths pass through the vegetation cover and are used to generate a DEM (Digital Elevation Model). The short wavelengths are reflected from the top of forest canopies and are used to generate a DSM (Digital Surface Model). Both models are thoroughly calibrated and have a spatial resolution (pixel size) of 2.5 m. The difference between the DSM and DEM is taken to represent height of vegetation (MURA *et al*., 2001; NEEFF *et al*., 2005b).

NEEFF *et al*. (2005b) depict interferometric height in primary forests as being dependent on only a sub-collective of the largest trees of the forest. Therefore, the canopy and the crown structure that can be recognized in the digital height model is a function of only the largest trees.

Sample blocks of undisturbed primary forest were extracted from the digital height model. Namely, three contiguous areas of 1,000 x 1,000 m = 100 ha each were selected, that are reasonably far away from roads etc.

### 2.3 Local maximum filtering

Local maximum filtering (LM filtering) extracts tree locations from remote sensing imagery. Even though many other approaches have been proposed, LM filtering has yielded good results, is fairly simple to implement, and has therefore been used extensively (WULDER *et al*., 2000). In LM filtering, a pixel window is passed over an image, to determine for each pixel, whether its digital number is higher than all other pixels in the window. These local maxima are identified as tree locations. The application of LM filtering to a digital height model directly makes use of the three dimensional canopy structure of forests, where the areas of maximum vegetation height obviously coincide with the tops of crowns.

### 2.4 Spatial point patterns

The statistical methodology regarding the analysis of spatial point patterns, that is applied in this paper comes primarily from the book by CRESSIE (1993), from which most of the terminology is taken: A spatial point process is a stochastic model, that governs the location of events $s_i$ in some subset of $R^d$. In this paper we are interested in the realization of the process as a spatial point pattern of trees in the forest: $s_i \in A \subset R^2$.

Point processes are commonly characterized and analysed by their moment measures. The first-order intensity $\lambda$ corresponds to the number of events per unit area. The second-order intensity is usually addressed by the K-function, which effectively summarizes spatial dependence over a wide range of scales. Here an estimator $\hat{K}$ is used, that corrects for edge effects by a guard area:

$\lambda \cdot$ K(h) = E(# extra events within distance $h$ of a randomly chosen event), $h > 0$, (1)

$$\hat{K}(h) = \hat{\lambda}^{-1} \sum_{i=1}^{N^+} \sum_{j=1}^{N} \mathrm{I}(\| s_i - s_j \| \leq h)/\mathrm{N}$$

$$\mathrm{i} \neq \mathrm{j} \text{ and } \mathrm{h} > 0, \qquad (2)$$

where $||si - sj||$ is the distance between events $s_i$ and $s_j$; $I$ is an indicator function $I = \{1$ if $||s_i - s_j|| \leq h$, 0 otherwise$\}$; $N$ is the number of points in a bounded study region $A$, and $N^+$ is the number of events in $A$ and a surrounding guard area.

Parametric models for spatial point processes can be fitted to observed point patterns. Here, the so-called Markov processes are used to describe the observed spatial pattern of very large trees in primary forests. Markov processes are appropriate for describing the point pattern of old growth forests because VLT spacing tends to be more uniform than clustered. This happens because the very large trees effectively outcompete other vegetation in a circular zone surrounding each VLT. An observed spatial point process in $A$ is Markov of range $\rho$ if the conditional intensity at $s_i$, depends only on the events in the circle of radius $\rho$ centered at $s_i$ (excluding $s_i$ itself). These models are most commonly used to model repulsive interaction that leads to a regular point pattern. Two events interact and are called neighbors if their distance $h_{ij} = ||s_i - s_j||$ is

less than $\rho$. It is convenient to describe the interaction structure of the process in terms of pair-potential functions, that usually are functions of the distance $h$ only (for simplicity used here instead of $h_{ij}$ for the distance between two points $i$ and $j$) $\Psi(s_i, s_j) = \Psi(h_{ij})$. Pair-potentials range from $\Psi(h) < 0$ (attraction) over $\Psi(h) = 0$ (independence) to $\Psi(h) > 0$ (inhibition), where $\Psi(h) = \infty$ corresponds to complete inhibition. The distribution of a point process is often described in terms of its likelihood $l(\theta)$, given its parameters $\theta$:

$$l(\theta \mid \{s_1, \ldots, s_n\}) \propto \exp\left\{\sum_{i=1}^{n} \log \beta - \sum_{1<i<j<n}\sum \Psi(h_{ij})\right\}, \quad (3)$$

where $n$ is the number of points, and $\beta$ reflects the first order intensity of the process. So, the probability of observing two points $s_i$, $s_j$ at distance $h_{ij}$ apart is $e^{-\Psi(h_{ij})}$.

Some special cases of the Markov process include the Poisson process, which is the model of complete spatial randomness (CSR), the model of simple sequential inhibition (SSI), the Strauss process (Strauss), a Strauss hard-core model (StrHC), and a soft-core process (SC), which are given by (for simplicity, again $h$ is used instead of $h_{ij}$ for the distance between two points $i$ and $j$, the $\rho$, $\gamma$, $\sigma$, $\kappa$ are the parameters of the respective functions):

$$\Psi_{CSR}(h) = 0, \quad (4)$$

$$\Psi_{SSI}(h) = \begin{cases} \infty, & 0 < h \le \rho, \\ 0, & h > \rho, \end{cases} \quad (5)$$

$$\Psi_{Strauss}(h) = \begin{cases} -\log\gamma, & 0 < h \le \rho, \\ 0, & h > \rho, \end{cases} \quad (6)$$

$$\Psi_{StrHC}(h) = \begin{cases} \infty, & 0 < h \le \rho_0, \\ -\log\gamma, & \rho_0 < h \le \rho_1, \\ 0, & h > \rho_1, \end{cases} \quad (7)$$

$$\Psi_{SC}(h) = \left(\frac{\sigma}{h}\right)^{\frac{2}{\kappa}}, \quad 0 < \kappa < 1. \quad (8)$$

## 3. RESULTS

### 3.1 Extraction of tree locations from digital height model

LM filtering was used to extract the positions of very large trees from the DHM. LM filtering by an approximation of a circular window with radius of three pixels (= 7.5 m) yielded particularly good results. Tree locations are marked at those points in the images were characteristic maxima are observable, that most probably coincide with crowns of trees. Because of the cost of conducting a field based survey of tree locations, we were unable to fully assess the accuracy of the derived tree positions using the image methods described previously. Based on our experience in this forest type, and also based on visual examination we judged this method to provide sufficient accuracy for the purpose of conducting exploratory point pattern analysis. Visual examination of the results justifies the approach adopted for selection of filter size. The resulting spatial point patterns are displayed in Figure 1. Intuitively, the pattern does not seem to contain clusters, but rather to be fairly regular.

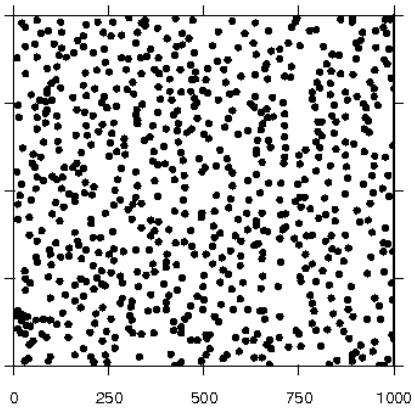


Fig. 1 – Spatial pattern of very large trees in sample block #1. Plot area covers 1000 x 1000 m = 100 ha.

### 3.2 Distance between very large trees

The spatial point patterns from LM filtering of the sample blocks are analyzed by simple summary statistics. The intensities of the VLT point patterns are estimated as $\lambda_1$ = 6.91 ha$^{-1}$, $\lambda_2$ = 6.51 ha$^{-1}$, and $\lambda_3$ = 6.78 ha$^{-1}$. For each tree, the distance to its nearest neighbor is computed. The mean distances for the three blocks turn out to be very similar: $\bar{W}_1$ = 24.2 m, $\bar{W}_2$ = 25.1 m, $\bar{W}_3$ = 24.2 m. Since $\lambda_1$ and $\bar{W}_i$ from the different blocks are very similar, the spatial pattern, at least at small scales, can be considered homogeneous.

### 3.3 Modeling of point patterns

Markov point processes are fitted to the point patterns as resulting from the LM filtering of the DHM. No maximum likelihood estimators are available for the Strauss process (Strauss), the Strauss hard-core model (StrHC), or the soft-core process (SC). The fitting procedure maximizes the pseudolikelihood (MPL) and utilizes the tools given in the *spatstat 1.2* library of R. The parameters of the homogeneous Poisson process (CSR) and the model of simple sequential inhibition (SSI) are fitted by their maximum likelihood estimators.

TABLE 1 – COEFFICIENTS OF FITTED MODELS FOR SPATIAL POINT PATTERNS IN THREE SAMPLE BLOCKS. CONSIDERED MODELS ARE: CSR – HOMEOGENEOUS POISSON PROCESS, SSI – SIMPLE SEQUENTIAL INHIBITION, STRAUSS – HOMOGENEOUS STRAUSS PROCESS, StrHc – STRAUSS HARD-CORE, SC – SOFT-CORE.

| Model | Parameter | block #1 | block #2 | block #3 |
|---|---|---|---|---|
| CSR | $\lambda$ | 0.000691 | 0.000651 | 0.000651 |
| | $\gamma$ | 1 | 1 | 1 |
| SSI | $\beta$ | 0.0007575 | 0.00071 | 0.0007445 |
| | $\rho$ | 9 | 9 | 9 |
| | $\gamma$ | 0 | 0 | 0 |
| Strauss | $\beta$ | 0.0007575 | 0.00071 | 0.0007445 |
| | $\rho$ | 10 | 10 | 10 |
| | $\gamma$ | 0.1322 | 0.1227 | 0.1327 |
| StrHC | $\beta$ | 0.001029 | 0.001007 | 0.0009785 |
| | $\rho_0$ | 9 | 9 | 9 |
| | $\rho_1$ | 30 | 30 | 29 |
| | $\gamma_0$ | 0 | 0 | 0 |
| | $\gamma_1$ | 0.7963 | 0.7456 | 0.7907 |
| SC | $\beta$ | 0.0008028 | 0.0007245 | 0.0007629 |
| | $\sigma$ | 10.82 | 15.27 | 13.68 |
| | $\kappa$ | 0.359 | 0.2564 | 0.2821 |

Model Selection between different parametrizations (different values of $\rho_i$ and $\kappa$) for the Strauss, the StrHC, and the SC models, is done by fitting a series of models. The estimates for MPL of different parameter combinations were compared and those with the highest pseudolikelihood values were selected. An example curve of the MPL of the SC model in the three blocks is displayed in Figure 2. The parameters for all final models are displayed in Table 1 for the three point patterns. The parameter estimates are similar between the sample blocks.

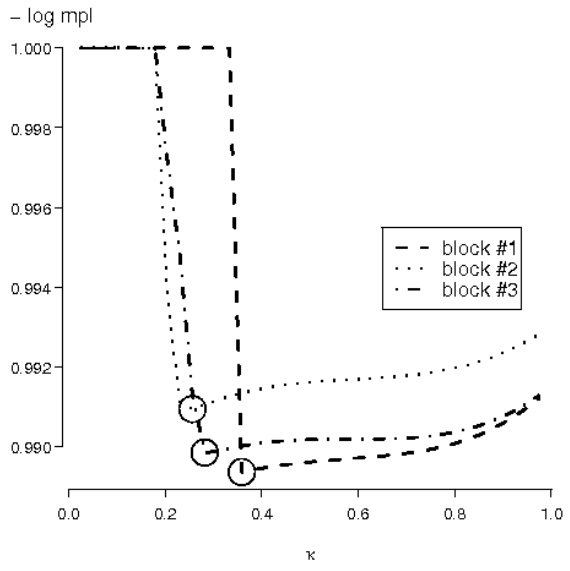


Fig. 2 – Fitting of a soft-core model to the observed point patterns in sample blocks #1-3. Displayed are the negative log-pseudolikelihood (mpl) curves for different parametrizations of the soft-core models by their interaction parameter κ. Minima (final model) are marked by circles. All values are scaled by 1 / max{-log $mpl_i$} for visual comparison.

Assessment of the fitted models draws on the empirical and the theoretical K-functions of the processes, and on Monte-Carlo simulations. In most cases expressions for the theoretical K-function are available as well, and then empirical and theoretical K-functions can be compared to see the general fit of the model to the data. In the Monte-Carlo approach, repeated simulation of a point pattern with the parameters from model fit yields a series of patterns with associated simulated empirical K-functions. These series provide confidence intervals for the true K-function, given a particular point processes model fits the data (see Figure 3). The K-functions for models of CSR, SSI, Strauss and StrHC are displayed in Figure 3. All four models fit the data well for larger scales at $h$= 50-75 m, all of them display asymptotes of CSR that the functions approach from below. However, at lower scales the K-functions exceed the confidence intervals. Thus, these models do not provide a satisfactory fit to the data; fit is particularly important at lower scales. Among these 4 models, the Strauss hard-core fit the data the best. There were significant deviations from the Strauss hard-core confidence intervals for distances under 30 m, but the deviations were of a much smaller magnitude than with the other three models. However, there was still a significant amount of regularity that was not explained by this model at distances less than 30 m.

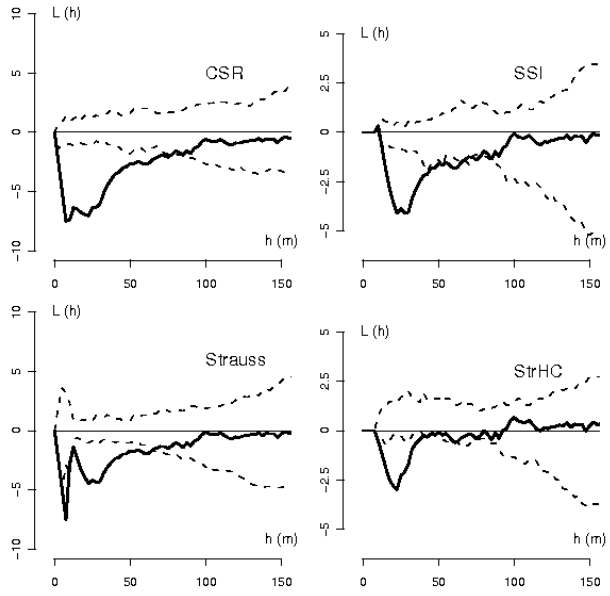


Fig. 3 – K-functions of sample block #1 for various point process models. Legend: CSR - homogeneous Poisson process, SSI - simple sequential inhibition, Strauss - homogeneous Strauss process, and StrHC - Strauss hard-core. All functions are transformed by the theoretical K-functions of their respective processes to $L = K^{-1} - h$, e.g. $L_{CSR} = \sqrt{K_{CSR}/\pi} - h$. The bold solid lines are the empirical K-functions, the solid (non-bold), horizontal line is the theoretical K-function, and the dotted lines correspond to the confidence intervals from Monte-Carlo simulation ($\alpha = 0.1$, $n = 20$), given the fitted models.

The SC model (Figure 4) is the model that fits the data best. The K-functions in Figure 3 all provided evidence of strong regularity at scales less than 50 m, that was not accounted for by the models tested. The degree of regularity decreased with increasing distance. Therefore, we expect that the soft-core inhibition model will be superior because it lets the interaction continuously decrease with distance. The K-functions for all three plots are displayed in Figure 4. In all three cases, the empirical K-function remains within the confidence intervals from Monte-Carlo simulation over the whole range of distances. Apparently, the soft-core pair potential function was a feasable representation of the point pattern for all three image blocks. This model may prove useful in characterizing the point pattern of VLTs for other forest types and locations in Amazonia.

## 4. DISCUSSION

Very large trees in the Amazon forest are of utmost importance for forest structure. Because of their large size and dominant position in the forest, the VLTs can be detected by radar remote sensing, and a relatively simple approach of LM filtering allows us to extract their locations from a digital model of forest height. These locations form a spatial point pattern, that is analysed using spatial statistics.

Exploratory statistics describe a sub-collective of only seven trees per hectare, that contain a huge fraction of the forest's above-ground biomass. They form a fairly regular pattern, and have an average spacing of ca. 24 m (see Figure 1). Modeling of the spatial point patterns by Markov processes reveals a certain repulsion between neighboring VLTs. So, given one VLT, it is very improbable to find another very large tree close by, because individuals would inhibit each other. The preference of a soft-core model (SC) over the alternatives suggests that this repulsion is a function of distance; locations of very large trees are almost independent only at distances above ca. 29 m. Moreover, the repulsive dependence is shown to decrease smoothly with distance. Therefore, it is possible to find VLTs in close proximity: it is just extremely unlikely.

Very large trees have been described in the literature as drivers of forest sucession by the mechanism of gap formation and regeneration in gaps when one of the huge individuals eventually falls (Brokaw, 1982). These processes, i.e. natural degradation and regeneration, can be deduced to happen at a scale of about 24 m, that corresponds to the spacing of the VLTs.

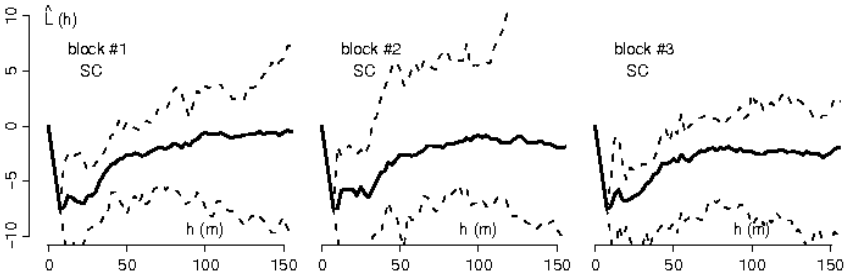


Fig. 4 – K-functions of final model in all three sample blocks. Solid lines correspond to empirical K-functions, dotted lines are confidence intervals from Monte-Carlo simulation $\alpha = 0.1$, $n = 20$), given the fitted soft-core model (SC). All functions are transformed for display purposes by the theoretical K-function under CSR to $L = \sqrt{K_{CSR}/\pi} - h$.

**ACKNOWLEDGEMENTS**

The authors acknowledge CNPq (grant #'s 382660/02-1, 309922/03-8(PV), 300677/91-0, 380597/99-3, 300927/92-4) support.

**REFERENCES**

BROKAW, N. The definition of treefall gap and its effect on measures of forest dynamics. **Biotropica**, v. 14, n. 2, p. 158–160, 1982.

CHAMBERS, J.; SANTOS, J.; RIBEIRO, R.; HIGUCHI, N. Tree damage, allometric relationships, and above-ground net primary production in central Amazon forest. **Forest Ecology and Management**, v. 152, p. 73–84, 2001.

CRESSIE, N. **Statistics for spatial data**. New York: John Wiley & Sons, 1993.

MILTON, K.; LACA, E.; DEMMENT, M. Successional patterns of mortality and growth of large trees in a Panamanian lowland forest. **Journal of Ecology**, v. 82, n. 1, p. 79–87, 1994.

MURA, J. C.; BINS, L. S.; GAMA, F. F.; FREITAS, C. C.; SANTOS, J. R.; DUTRA; L. V., Identification of the Tropical Forest in Brazilian Amazon based on the DEM difference from P and X bands interferometric data, International Geoscience and Remote Sensing Symposium (IGARSS), Sidney, July 2001. **Anais**. 2001.

NEEFF, T.; DUTRA, L. V.; DOS SANTOS, J. R.; FREITAS, C. C.; ARAUJO, L. S. Power spectrum analysis of SAR data for remote sensing of spatial forest structure in Brazilian Amazon. **International Journal of Remote Sensing**, accepted, 2005a.

NEEFF, T.; DUTRA, L. V.; DOS SANTOS, J. R.; FREITAS, C. C.; ARAUJO, L. V. Tropical forest measurement by interferometric height modelling and P-band radar backscatter. **Forest Science**, accepted, 2005b.

PRETZSCH, H. Analysis and modeling of spatial stand structures. Methodological considerations based on mixed beech-larch stands in Lower Saxony. **Forest Ecology and Management**, v. 97, p. 237–253, 1997.

STOYAN, D.; PENTTINEN, A. Recent applications of point process methods in forestry statistics. **Statistical Science**, v. 15, n. 1, p. 61–78, 2000.

WULDER, M.; NIEMANN, K.; GOODENOUGH, D. Local maximum filtering for the extraction of tree locations and basal area from high spatial resolution imagery. **Remote Sensing of the Environment**, v. 73, p. 103–114, 2000.